

RUSSIAN ACADEMY OF SCIENCE
Lenin Order of Siberian Branch
G.I. BUDKER INSTITUTE OF NUCLEAR PHYSICS

V.N. Baier and V.M. Katkov

SPECTRUM AND POLARIZATION
OF COHERENT AND INCOHERENT
RADIATION AND THE LPM EFFECT
IN ORIENTED SINGLE CRYSTAL

Budker INP 2007-22

Novosibirsk
2007

**Spectrum and polarization
of coherent and incoherent radiation
and the LPM effect in oriented single crystal**

V.N. Baier and V.M. Katkov

Institute of Nuclear Physics
630090, Novosibirsk, Russia

Аннотация

The spectrum and the circular polarization of radiation from longitudinally polarized high-energy electrons in oriented single crystal are considered using the method which permits inseparable consideration of both the coherent and the incoherent mechanisms of photon emission. The spectral and polarization properties of radiation are obtained and analyzed. It is found that in some part of spectral distribution the influence of multiple scattering (the Landau-Pomeranchuk-Migdal (LPM) effect) attains the order of 7 percent. The same is true for the influence of multiple scattering on the polarization part of the radiation intensity. The degree of circular polarization of total intensity of radiation is found. It is shown that the influence of multiple scattering on the photon polarization is similar to the influence of the LPM effect on the total intensity of radiation: it appears only for relatively low energies of radiating electron and has the order of 1 percent, while at higher energies the crystal field action excludes the LPM effect.

1 Introduction

The study of processes with participation of polarized electrons and photons permits to obtain the important physical information. Because of this reason the experiments with use of polarized particles are performed and are planning in many laboratories (CERN, Jefferson Nat Accl Fac, SLAC, BINP, etc). In this paper the polarization effects are considered in the frame of general theory developed by authors [1], which includes both the coherent and the incoherent mechanisms of radiation from high-energy electrons in an oriented single crystal. The influence of multiple scattering on the radiation process including polarization effects is analyzed. The study of radiation in oriented crystals is continuing and new experiments are performed recently see [2], [3].

The general expression for the energy loss of the longitudinally polarized electron in oriented crystal was found in [4] (see Eq.(2.7))

$$dE_\xi = -\frac{\alpha m^2}{8\pi^2} \frac{d^3k}{\varepsilon \varepsilon'} \int \frac{d^3r}{V} F(\mathbf{r}, \vartheta_0) \int e^{-iA} \left[\varphi_1(\xi) + \frac{1}{4} \varphi_2(\xi) \gamma^2 (\mathbf{v}_1 - \mathbf{v}_2)^2 \right] dt_1 dt_2,$$

$$A = \frac{\omega \varepsilon}{2\varepsilon'} \int_{t_1}^{t_2} \left[\frac{1}{\gamma^2} + (\mathbf{n} - \mathbf{v}(t))^2 \right] dt,$$

$$\varphi_1(\xi) = 1 + \xi \frac{\omega}{\varepsilon}, \quad \varphi_2(\xi) = (1 + \xi) \frac{\varepsilon}{\varepsilon'} + (1 - \xi) \frac{\varepsilon'}{\varepsilon}. \quad (1.1)$$

where $dE_\xi = \omega dw_\xi$, dw_ξ is the probability of radiation, see e.g. Eq.(4.2) in [5], ω and ε are the photon and electron energy, $\alpha = e^2 = 1/137$, the vector \mathbf{k} is the photon momentum, $\mathbf{n} = \mathbf{k}/|\mathbf{k}|$, $\xi = \lambda\zeta$, $\lambda = \pm 1$ is the helicity of emitted photon, $\zeta = \pm 1$ is the helicity of the initial electron, $F(\mathbf{r}, \vartheta_0)$ is the distribution function of electron in the transverse phase space depending on the angle of incidence ϑ_0 of the electron on crystal, $\mathbf{v}_1 = \mathbf{v}(t_1)$ is the electron velocity (see [5], Sec.16.2).

The degree of the circular polarization of radiation is defined by Stoke's parameter ξ_2 :

$$\xi_2 = \Lambda(\zeta \mathbf{v}), \quad \Lambda = \frac{dE_+ - dE_-}{dE_+ + dE_-}, \quad (1.2)$$

where the quantity $(\zeta \mathbf{v})$ defines the longitudinal polarization of the initial electrons, dE_+ and dE_- is the energy loss for $\xi=+1$ and $\xi=-1$ correspondingly.

It should be noted that a few different spin correlations are known in an external field. But after averaging over directions of crystal field only the considered here longitudinal polarization survives.

In [4] the polarization effects in the coherent radiation which dominates at high electron energies ($\varepsilon \gg 1$ GeV for main axes of heavy elements, e.g. tungsten crystal) was studied. At intermediate energies the incoherent radiation contributes essentially and the contributions of both mechanisms should be taken into account. Recently authors developed the method which permits indivisible consideration of both the coherent and the incoherent mechanisms of photon emission in oriented crystals [1].

Basing on Eqs.(18) and (19) of [1] (see also Eqs. (7.89) and (7.90) in [5]) and using Eq.(1.1) one can obtain the general expression for the intensity of radiation from longitudinally polarized electrons which includes the coherent and incoherent contributions and the Landau-Pomeranchuk-Migdal (LPM) effect:

$$dI_\xi(\varepsilon, y) = dI_0(\varepsilon, y) + \xi dI_1(\varepsilon, y) = \frac{\alpha m^2}{2\pi} \frac{y dy}{1-y} \int_0^{x_0} \frac{dx}{x_0} G_{r\xi}(x, y),$$

$$G_{r\xi}(x, y) = \int_0^\infty F_{r\xi}(x, y, t) dt - r_{3\xi} \frac{\pi}{4},$$

$$F_{r\xi}(x, y, t) = \text{Im} \left\{ e^{i\varphi_1(t)} [r_{2\xi} \nu_0^2 (1 + ib_r) \varphi_2(t) + r_{3\xi} \varphi_3(t)] \right\}, \quad b_r = \frac{4\chi^2(x)}{u^2 \nu_0^2},$$

$$y = \frac{\omega}{\varepsilon}, \quad u = \frac{y}{1-y}, \quad \varphi_1(t) = (i-1)t + b_r(1+i)(\varphi_2(t) - t),$$

$$\varphi_2(t) = \frac{\sqrt{2}}{\nu_0} \tanh \frac{\nu_0 t}{\sqrt{2}}, \quad \varphi_3(t) = \frac{\sqrt{2} \nu_0}{\sinh(\sqrt{2} \nu_0 t)}, \quad (1.3)$$

where

$$r_{2\xi} = \frac{1}{2} (r_2 + \xi r_{21}), \quad r_2 = 1 + (1-y)^2, \quad r_{21} = 2y - y^2$$

$$r_{3\xi} = \frac{1}{2} (r_3 + \xi r_{31}), \quad r_3 = 2(1-y), \quad r_{31} = 2y(1-y),$$

$$\nu_0^2 = \frac{1-y}{y} \frac{\varepsilon}{\varepsilon_c(x)}, \quad (1.4)$$

The intensity for unpolarized electrons $dI_0(\varepsilon, y)$ was obtained in [1], the polarization term $dI_1(\varepsilon, y)$ is found here.

The situation is considered when the electron angle of incidence ϑ_0 (the angle between electron momentum \mathbf{p} and the axis (or plane)) is small $\vartheta_0 \ll V_0/m$. The axis potential (see Eq.(9.13) in [5]) is taken in the form

$$U(x) = V_0 \left[\ln \left(1 + \frac{1}{x + \eta} \right) - \ln \left(1 + \frac{1}{x_0 + \eta} \right) \right], \quad (1.5)$$

where

$$x_0 = \frac{1}{\pi d n_a a_s^2}, \quad \eta_1 = \frac{2u_1^2}{a_s^2}, \quad x = \frac{\varrho^2}{a_s^2}, \quad (1.6)$$

Here ϱ is the distance from axis, u_1 is the amplitude of thermal vibration, d is the mean distance between atoms forming the axis, a_s is the effective screening radius of the potential. The parameters in Eq.(1.5) were determined by means of fitting procedure.

The local value of parameter $\chi(x)$ which determines the radiation probability in the field Eq.(1.5) is

$$\chi(x) = -\frac{dU(\varrho)}{d\varrho} \frac{\varepsilon}{m^3} = \chi_s \frac{2\sqrt{x}}{(x + \eta)(x + \eta + 1)}, \quad \chi_s = \frac{V_0 \varepsilon}{m^3 a_s} \equiv \frac{\varepsilon}{\varepsilon_s}. \quad (1.7)$$

For an axial orientation of crystal the ratio of the atom density $n(\varrho)$ in the vicinity of an axis to the mean atom density n_a is (see [1])

$$\frac{n(x)}{n_a} = \xi(x) = \frac{x_0}{\eta_1} e^{-x/\eta_1}, \quad \varepsilon_0 = \frac{\varepsilon_e}{\xi(0)}, \quad \varepsilon_e = \frac{m}{16\pi Z^2 \alpha^2 \lambda_c^3 n_a L_0}. \quad (1.8)$$

The functions and values in Eqs.(1.3) and (1.4) are

$$\begin{aligned} \varepsilon_c(x) &= \frac{\varepsilon_e(n_a)}{\xi(x)g(x)} = \frac{\varepsilon_0}{g(x)} e^{x/\eta_1}, \quad L_0 = \ln(ma) + \frac{1}{2} - f(Z\alpha), \\ g(x) &= g_0 + \frac{1}{6L_0} \left[\ln \left(1 + \frac{\chi^2(x)}{u^2} \right) + \frac{6D_{sc}\chi^2(x)}{12u^2 + \chi^2(x)} \right], \\ g_0 &= 1 + \frac{1}{L_0} \left[\frac{1}{18} - h \left(\frac{u_1^2}{a^2} \right) \right], \quad a = \frac{111Z^{-1/3}}{m}, \quad f(\xi) = \sum_{n=1}^{\infty} \frac{\xi^2}{n(n^2 + \xi^2)}, \\ h(z) &= -\frac{1}{2} [1 + (1+z)e^z \text{Ei}(-z)], \end{aligned} \quad (1.9)$$

where the function $g(x)$ determines the effective logarithm using the interpolation procedure: $L = L_0 g(x)$, see Eq.(14) in [1], $D_{sc} = 2,3008$ is the constant entering in the radiation spectrum at $\chi/u \gg 1$, see Eq.(7.107) in [5], $\text{Ei}(z)$ is the integral exponential function, $f(\xi)$ is the Coulomb correction.

It follows from Eqs.(1.2) and (1.3) that the circular polarization of radiation is

$$\xi_2 = \frac{dI_1(\varepsilon, y)}{dI_0(\varepsilon, y)}(\zeta\mathbf{v}), \quad (1.10)$$

2 The spectral distribution of radiation

The expression for dI_ξ Eq.(1.3) includes both the coherent and incoherent contributions as well as the influence of the multiple scattering (the LPM effect) on the photon emission process.

The probability of the coherent radiation $dI_0^{coh}(\varepsilon, y)$ is the first term ($\nu_0^2 = 0$) of the decomposition of Eq.(1.3) over ν_0^2 . This probability is contained in Eq.(17.7) of [5]. The polarization term in the probability of the coherent radiation $dI_1^{coh}(\varepsilon, y)$ is the first term of the decomposition of dI_1 in Eq.(1.3) over ν_0^2 . The expression $dI_0^{coh} + \xi dI_1^{coh}$ coincides with the term containing $R_0(\lambda)$ in Eq.(3.5) of [4].

The intensity of the incoherent radiation $dI_0^{inc}(\varepsilon, y)$ is the second term ($\propto \nu_0^2$) of the mentioned decomposition of $dI(\varepsilon, y)$ [1]. The expression for $dI_0^{inc}(\varepsilon, y)$ follows also from Eq.(21.21) in [5]). The polarization term $dI_1^{inc}(\varepsilon, y)$ is correspondingly the second term ($\propto \nu_0^2$) of decomposition of $dI_1(\varepsilon, y)$:

$$dI_{0,1}^{inc}(\varepsilon, y) = \frac{\alpha m^2 \varepsilon}{60\pi \varepsilon_0} \int_0^{x_0} g(x) e^{-x/\eta_1} dJ_{0,1}^{inc}(\chi, y) \frac{dx}{x_0}, \quad (2.1)$$

here $\chi = \chi(x)$, the notations is given in Eqs.(1.7), (1.8) and (1.9), $dJ_{0,1}^{inc}(\chi)$ can be written as

$$\begin{aligned} dJ_0^{inc}(\chi, y) &= [y^2(f_1(z) + f_2(z)) + 2(1-y)f_2(z)] dy, \\ dJ_1^{inc}(\chi, y) &= [y^2(f_1(z) - f_2(z)) + 2yf_2(z)] dy, \\ z &= \left(\frac{y}{\chi(1-y)} \right)^{2/3}, \end{aligned} \quad (2.2)$$

the functions $f_1(z)$ and $f_2(z)$ are defined in the just mentioned equation in [5]:

$$\begin{aligned} f_1(z) &= z^4\Upsilon(z) - 3z^2\Upsilon'(z) - z^3, \\ f_2(z) &= (z^4 + 3z)\Upsilon(z) - 5z^2\Upsilon'(z) - z^3, \end{aligned} \quad (2.3)$$

here $\Upsilon(z)$ is the Hardy function:

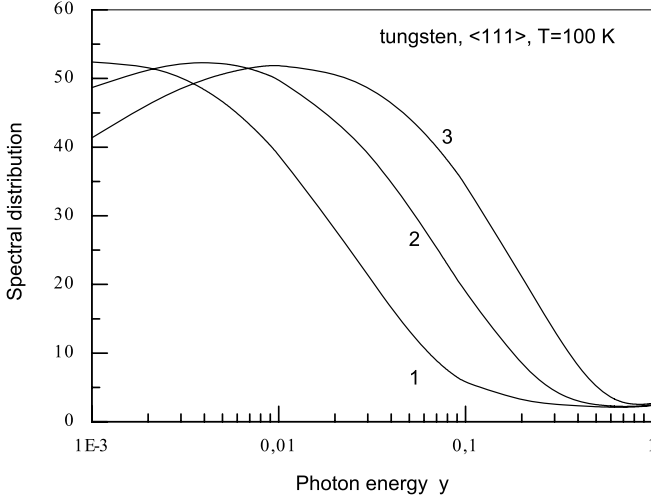


Fig. 1: The spectral distribution of radiation in tungsten, axis $\langle 111 \rangle$, temperature $T=100$ K, with taking into account all mechanisms of photon emission. The spectral inverse radiation length (in cm^{-1}) $dI_0(\varepsilon, y)/\varepsilon dy$, see Eq.(1.3), is shown vs $y = \omega/\varepsilon$ for different energies: curve 1 is for $\varepsilon = 0.3$ GeV, curve 2 is for $\varepsilon = 1$ GeV and curve 3 is for $\varepsilon = 3$ GeV.

$$\Upsilon(z) = \int_0^{\infty} \sin\left(z\tau + \frac{\tau^3}{3}\right) d\tau. \quad (2.4)$$

For intermediate energies, where both the coherent and the incoherent contributions to the total intensity of radiation are essential, the spectral distribution of intensity $dI_0(\varepsilon, y)$ is shown in Fig.1. The calculation was done for axis $\langle 111 \rangle$ of tungsten at low temperature $T=100$ K (see Table 1, the parameters are defined above, ε_t is introduced in [1]). These spectra describe radiation in thin targets when one can neglect the energy loss of projectile. It is seen that the phenomena under consideration become apparent at relatively

Table 1. Parameters of radiation process of the tungsten crystal, axis $\langle 111 \rangle$ and germanium crystal, axis $\langle 110 \rangle$ for two temperatures T .

Crystal	T(K)	$V_0(\text{eV})$	x_0	η_1	η	$\varepsilon_0(\text{GeV})$	$\varepsilon_t(\text{GeV})$	$\varepsilon_s(\text{GeV})$	h
W	293	417	39.7	0.108	0.115	7.43	0.76	34.8	0.348
W	100	355	35.7	0.0401	0.0313	3.06	0.35	43.1	0.612
Ge	293	110	15.5	0.125	0.119	148	1.29	210	0.235
Ge	100	114.5	19.8	0.064	0.0633	59	0.85	179	0.459

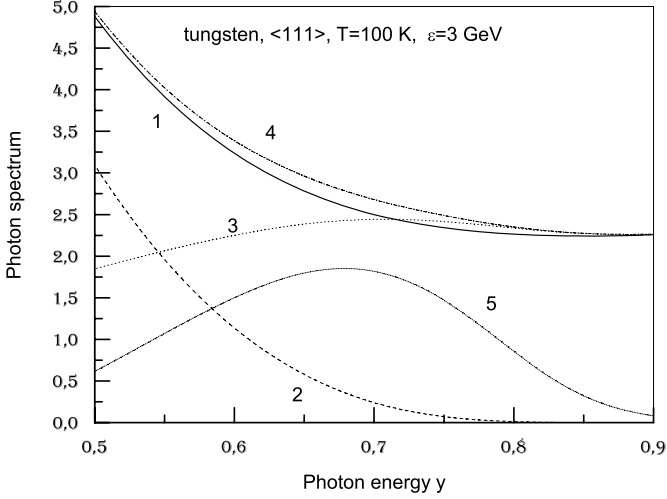


Рис. 2: The different contributions to the photon spectrum for electron energy $\varepsilon = 3$ GeV, axis $\langle 111 \rangle$, temperature $T=100$ K. The curve 1 is $dI_0(\varepsilon, y)$, the curve 2 is the coherent spectrum $dI_0^{coh}(\varepsilon, y)$, the curve 3 is the incoherent spectrum $dI_0^{inc}(\varepsilon, y)$, the curve 4 is the sum $dI_0^{coh}(\varepsilon, y) + dI_0^{inc}(\varepsilon, y)$, and the curve 5 is the difference $10 (dI_0^{coh}(\varepsilon, y) + dI_0^{inc}(\varepsilon, y) - dI_0(\varepsilon, y))$.

low energy. For $\varepsilon = 0.3$ GeV, $dI_0^{coh} \simeq dI_0^{inc}$ at $y \simeq 0.1$ ($\omega \simeq 60$ MeV) while for lower photon energy the coherent contribution dominates and for higher photon energy the incoherent contribution dominates. For $\varepsilon = 1$ GeV, $dI_0^{coh} \simeq dI_0^{inc}$ at $y \simeq 0.28$ ($\omega \simeq 280$ MeV) and for $\varepsilon = 3$ GeV, $dI_0^{coh} \simeq dI_0^{inc}$ at $y \simeq 0.54$ ($\omega \simeq 1.6$ GeV). All spectrum curves have very steep (exponential) right slope the location of which is defined by the electron energy.

The next terms of decomposition of the intensity $dI_0(\varepsilon, y)$ over ν_0^2 describe the influence of multiple scattering on the radiation process, the LPM effect. The different contributions to that part of the spectrum, where the coherent and the incoherent contributions are comparable, are shown in Fig.2. The difference shown by curve 5 arises due to the LPM effect. We define the contribution of the LPM effect into spectral distribution, by analogy with [1], as

$$\Delta_s = -\frac{dI_0 - dI_0^{coh} - dI_0^{inc}}{dI_0}. \quad (2.5)$$

The function $\Delta_s(y)$ is shown in Fig.3. The curve 1 for $\varepsilon = 0.3$ GeV reaches the maximum 6.64 % at $y=0.18$, the curve 2 for $\varepsilon = 1$ GeV reaches the

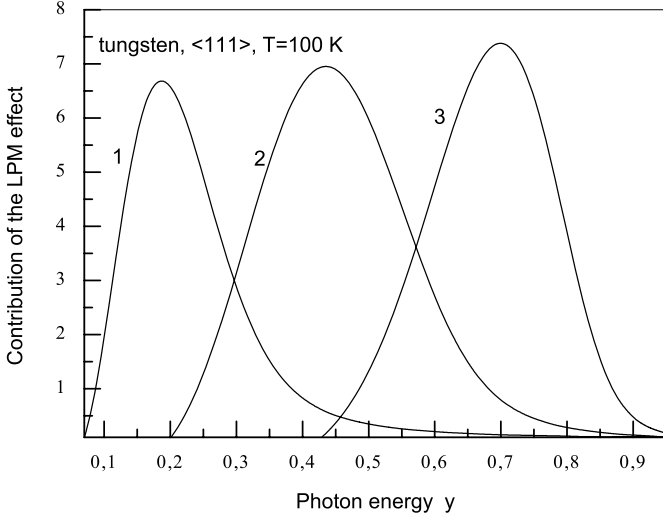


Рис. 3: The LPM effect for spectral distribution of radiation in tungsten, axis $\langle 111 \rangle$, temperature $T=100$ K. The function $\Delta_s(y)$ Eq.(2.5) is shown vs $y = \omega/\varepsilon$. Curve 1 is for $\varepsilon = 0.3$ GeV, curve 2 is for $\varepsilon = 1$ GeV and curve 3 is for $\varepsilon = 3$ GeV.

maximum 6.87 % at $y=0.44$ and the curve 3 for $\varepsilon = 3$ GeV reaches the maximum 7.32 % at $y=0.7$.

At room temperature ($T=293$ K) for axis $\langle 111 \rangle$ in tungsten for the electron energy $\varepsilon = 10$ GeV the different contributions to that part of the spectrum where the coherent and the incoherent contributions are comparable are shown in Fig.4. In this case the maximum of the function $\Delta_s(y) \simeq 6.03$ % is reached at $y=0.82$.

All the curves in Fig.3 have nearly the same height of the maximum and the position of the maximum is defined roughly by the expression $u_m \simeq 3\varepsilon/\varepsilon_0$ ($u \equiv y/(1-y)$). Such scaling in terms of u is the consequence of the following representation of the spectral inverse radiation length (the intensity spectrum Eq.(1.3))

$$\frac{dL_{rad}^{-1}}{dy} = \frac{1}{\varepsilon} \frac{dI_0(\varepsilon, y)}{dy} = r_2(y)R_2\left(\frac{\varepsilon}{u}\right) + r_3(y)R_3\left(\frac{\varepsilon}{u}\right). \quad (2.6)$$

In the high energy limit $\varepsilon \gg \varepsilon_0$ the maximum of the LPM effect is situated at the very end of the spectrum. In this limit $r_2 \simeq 1 - O(\varepsilon_0/\varepsilon)$ and $r_3 \simeq O(\varepsilon_0/\varepsilon)$ and the scaling (dependence on the combination ε/u only) of each of the two

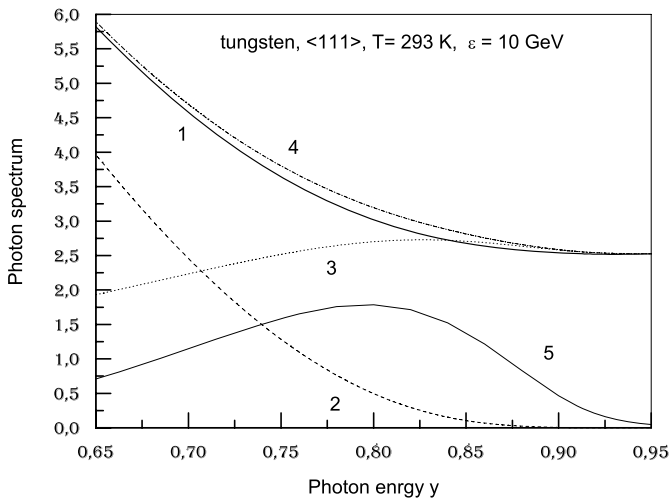


Рис. 4: the same as in Fig.2 but for $T=293$ K.

$R_{2,3}$ terms gets over into scaling of the whole expression for the spectral inverse radiation length.

In the maximum of the LPM effect the coherent contribution into spectral radiation intensity is relatively small: less than 10%. Therefore the right slope of curves in Fig.3 is described by formulas of the LPM effect in a medium (incoherent radiation) with corrections due to action of the crystal field. Far from the maximum at $u \gg \varepsilon/\varepsilon_0$ one has $R_{2,3}^{coh} = 0$ and the terms $\propto \nu_0^6$ in the decomposition of the functions $R_{2,3}$ (which includes the crystal field corrections) have the form

$$\Lambda_2 = \frac{\varepsilon^2 g_0^2}{3\varepsilon_0^2 u^2} \left(1 + 377 \frac{\overline{\chi^2}}{u^2} \right), \quad \Lambda_3 = -\frac{\varepsilon^2 g_0^2}{3\varepsilon_0^2 u^2} \left(\frac{31}{63} + \frac{2704}{15} \frac{\overline{\chi^2}}{u^2} \right)$$

$$\Lambda_s = \frac{R_s^{inc} - R_s}{R_s^{inc}(\chi = 0)}, \quad \overline{\chi^2} = \int_0^\infty \chi^2(x) e^{-3x/\eta_1} \frac{dx}{\eta_1}. \quad (2.7)$$

Here the terms independent on field coincide with corresponding terms in Eq.(3.6) in [6], the corrections depending on crystal field are calculated in this paper. At the left slope of the curves in Fig.3 the coherent contribution dominates (see Fig.1), the relative contribution of incoherent radiation diminishes and the LPM effect is only its small part.

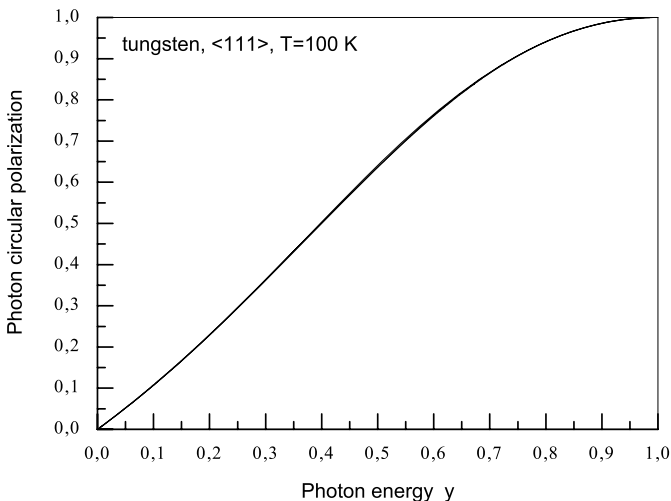


FIG. 5: Degree of the circular polarization of radiation in tungsten, axis $\langle 111 \rangle$, temperature $T=100$ K. The value of $\xi_2(y)$ Eq.(1.10) is shown vs $y = \omega/\varepsilon$. The curves for $\varepsilon = 0.3, 1, 3$ GeV coincide.

Degree of the circular polarization of radiation Eq.(1.10) is shown in Fig.5. The curves for energies $\varepsilon = 0.3, 1, 3$ GeV coincide with each other inside thickness of line. For any mechanism of radiation $\xi_2 \simeq y(\zeta \mathbf{v})$ for $y \ll 1$ (see Eq.(2.9)) in [4] and $\xi_2 \rightarrow 1$ for $y \rightarrow 1$ as a consequence of the helicity transfer from an electron to photon.

The next terms of decomposition of the intensity $dI_1(\varepsilon, y)$ over ν_0^2 describe the influence of multiple scattering on the polarization part of the spectral intensity of radiation. We define the contribution of this effect into the polarization part as

$$\Delta_{s1} = -\frac{dI_1 - dI_1^{coh} - dI_1^{inc}}{dI_1}. \quad (2.8)$$

The function $\Delta_{s1}(y)$ for $\varepsilon = 0.3$ GeV reaches the maximum 6.78 % at $y=0.18$, for $\varepsilon = 1$ GeV reaches the maximum 7.09 % at $y=0.44$ and for $\varepsilon = 3$ GeV reaches the maximum 7.43 % at $y=0.7$. It is seen that the maximum positions are situated at the same photon energy as in $\Delta_s(y)$ (see Fig.3) and their values are very close to these values in the unpolarized part. All this means that the multiple scattering is affecting similarly on the unpolarized spectrum described by $dI_0(\varepsilon, y)$ and the polarization term described by $dI_1(\varepsilon, y)$.

The influence of the multiple scattering on the photon polarization degree may be also characterized by

$$\Delta_{s\xi} = -\frac{\xi_{s2}^T - \xi_{s2}^{ci}}{\xi_{s2}^{ci}} = \Delta_{s1} - \Delta_s, \quad \xi_{s2}^T = \frac{dI_1(\varepsilon, y)}{dI_0(\varepsilon, y)}, \quad \xi_{s2}^{ci} = \frac{dI_1^{coh} + dI_1^{inc}}{dI_0^{coh} + dI_0^{inc}}. \quad (2.9)$$

Since value Δ_{s1} is very close to Δ_s the value of $\Delta_{s\xi}$ is much smaller than both Δ_s and Δ_{s1} .

3 Effect for the total intensity of radiation

Now we turn to analysis of the polarization effects for the total intensities of radiation

$$I_\xi(\varepsilon) = I_0(\varepsilon) + \xi I_1(\varepsilon), \quad I_0(\varepsilon) = \int_{y=0}^{y=1} dI_0(\varepsilon), \quad I_1(\varepsilon) = \int_{y=0}^{y=1} dI_1(\varepsilon). \quad (3.1)$$

The integral degree of the circular polarization of the radiation intensity in a crystal is given by the ratio $\xi_2^T = I_1(\varepsilon)/I_0(\varepsilon)$.

In [1] it was shown that the total intensity $I(\varepsilon)$ contains both the coherent and incoherent contributions as well as the influence of the multiple scattering (the LPM effect) on the process under consideration. The same is true for the polarization part $I_1(\varepsilon)$. The intensity of coherent radiation $I^F(\varepsilon) \equiv I_0^{coh}(\varepsilon)$ is the first term ($\nu_0^2 = 0$) of the decomposition of $I(\varepsilon)$ over ν_0^2 . Its explicit representation is given by Eqs.(25) and (26) in [1]. The coherent polarization part $I_1^{coh}(\varepsilon)$ is the first term ($\nu_0^2 = 0$) of the decomposition of $I_1(\varepsilon)$ over ν_0^2 . Both can be written in the form

$$I_{0,1}^{coh}(\varepsilon) = \int_0^{x_0} J_{0,1}^{coh}(\chi) \frac{dx}{x},$$

$$J_{0,1}^{coh}(\chi) = i \frac{\alpha m^2}{2\pi} \int_{\lambda-i\infty}^{\lambda+i\infty} \left(\frac{\chi^2}{3}\right)^s \Gamma(1-s) \Gamma(3s-1) (2s-1) a_{0,1} \frac{ds}{\cos \pi s},$$

$$a_0 = s^2 - s + 2, \quad a_1 = \frac{11}{6}(1-s), \quad \frac{1}{3} < \lambda < 1. \quad (3.2)$$

where $J_0^{coh}(\chi)$ is the radiation intensity and $J_1^{coh}(\chi)$ is the contribution of the circular polarization of radiation in external field (see Eqs.(4.50), (4.51) and (4.84) in [5]). The representation (3.2) is convenient both for the analytical

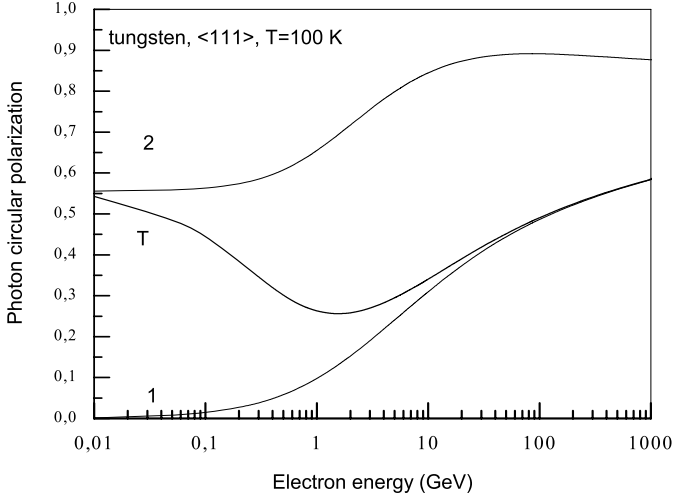


Рис. 6: The integral degree of the circular polarization in tungsten, axis $\langle 111 \rangle$, temperature $T=100$ K. The functions are shown vs electron energy in GeV. Curve 1 is for the coherent radiation ($\xi_2^{coh} = I_1^{coh}(\varepsilon)/I_0^{coh}(\varepsilon)$), curve 2 is for the incoherent radiation ($\xi_2^{inc} = I_1^{inc}(\varepsilon)/I_0^{inc}(\varepsilon)$), curve T is $\xi_2^T = I_1(\varepsilon)/I_0(\varepsilon)$ (see Eq.(3.1)).

and numerical calculation. The degree of circular polarization of the coherent radiation in a crystal we define by the ratio $\xi_2^{coh} = I_1^{coh}/I_0^{coh}$.

In [1] the new representation of the function $J_0^{inc}(\chi)$ was obtained, which is suitable for both analytical and numerical calculation. The same procedure can be applied to $J_1^{inc}(\chi)$. As a result we get

$$J_{0,1}^{inc}(\chi) = \frac{i\pi}{2} \int_{\lambda-i\infty}^{\lambda+i\infty} \frac{\chi^{2s} \Gamma(1+3s)}{3^s \Gamma(s)} R_{0,1}(s) \frac{ds}{\sin^2 \pi s}, \quad -\frac{1}{3} < \lambda < 0, \quad (3.3)$$

where

$$R_0(s) = 15 + 43s + 31s^2 + 28s^3 + 12s^4, \quad R_1(s) = \frac{25}{3} + 7s - \frac{109}{3}s^2 - 22s^3. \quad (3.4)$$

The integral degree of circular polarization of the incoherent radiation in a crystal we define by the ratio $\xi_2^{inc} = I_1^{inc}/I_0^{inc}$.

The integral degree of circular polarization in the tungsten crystal (axis $\langle 111 \rangle$, the temperatures $T=100$ K) $\xi_2^T = I_1(\varepsilon)/I_0(\varepsilon)$ Eq.(3.1) is shown

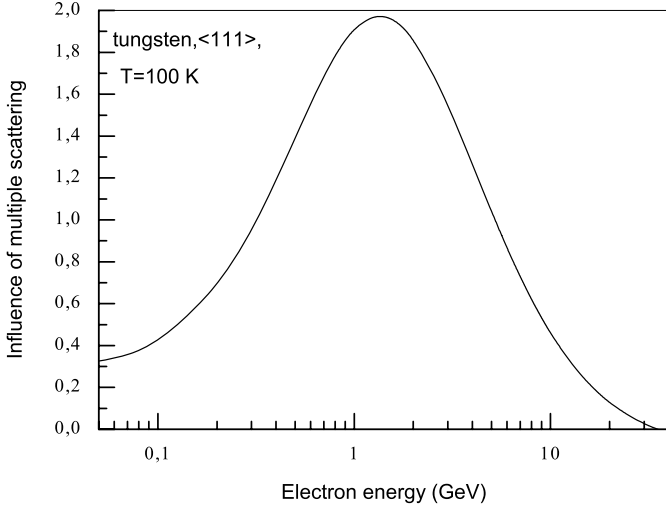


FIG. 7: Influence of multiple scattering on circular polarization of emitted radiation described by the function $\Delta_1(\varepsilon)$ Eq.(3.5) in tungsten, axis $\langle 111 \rangle$, temperature $T=100$ K.

in Fig.6 (the curve T), as well as the coherent degree $\xi_2^{coh} = I_1^{coh}/I_0^{coh}$ Eq.(3.2) (the curve 1) and the incoherent degree $\xi_2^{inc} = I_1^{inc}/I_0^{inc}$ Eq.(3.4) (the curve 2) as a function of incident electron energy ε . In low energy region ($\varepsilon \leq 1$ GeV) the contribution of incoherent mechanism dominates (let us remind that the intensities of the incoherent and coherent radiation become equal at $\varepsilon \simeq 0.4$ GeV). At higher energies the intensity $I_0^{coh}(\varepsilon)$ dominates while the intensity $I_0^{inc}(\varepsilon)$ decreases monotonically [1]. Correspondingly the curve ξ_2^{coh} tends to the curve ξ_2^T . At extremely high energy $\varepsilon > 10^6$ GeV ξ_2^{coh} tends to the external field limit: $\xi_2^{coh}=11/16$ (see Eq.(4.88) in [5]).

The next terms of decomposition of the total intensity $I(\varepsilon)$ over ν_0^2 describe the LPM effect in the radiation process. The contribution of the LPM effect in the total intensity of radiation I Eq.(3.1) is defined in [1] as $I^{LPM} = I_0 - I_0^{coh} - I_0^{inc}$. The relative contribution (negative since the LPM effect suppresses the radiation process) $\Delta = -I^{LPM}/I_0$ in the maximum is of the order of percent (see Fig.3 in [1]). Similarly we define the relative influence of multiple scattering on the photon integral circular polarization

as

$$\Delta_\xi = -\frac{\xi_2^T - \xi_2^{ci}}{\xi_2^{ci}} = \Delta_1 - \Delta, \quad \xi_2^{ci} = \frac{I_1^{coh} + I_1^{inc}}{I_0^{coh} + I_0^{inc}}, \quad \Delta_1 = \frac{I_1^{coh} + I_1^{inc}}{I_1} - 1. \quad (3.5)$$

The function of $\Delta_1(\varepsilon)$ (per cent) is shown in Fig.7, it attains the maximum $\Delta_1 \simeq 2.0\%$ at $\varepsilon \simeq 1.4$ GeV, while $\Delta_\xi(\varepsilon)$ attains the maximum $\Delta_\xi \simeq 1.4\%$ at $\varepsilon \simeq 1.8$ GeV and $\Delta(\varepsilon) \simeq 0.9\%$ at $\varepsilon \simeq 0.3$ GeV [1]. One can see that maxima of corresponding functions are slightly shifted with respect each other and the highest maximum has Δ_1 . From the other side, the behavior of all functions Δ , Δ_1 and Δ_ξ are quite similar: just as in the total intensity of radiation the suppression of integral polarization due to the multiple scattering is concentrated in the interval of moderate energies $\varepsilon < 10$ GeV and the scale of effect is of the order of percent.

4 Conclusion

In this paper the spectrum of radiation from an electron of intermediate energy (a few GeV for heavy elements) moving in oriented crystal is calculated for the first time. The interplay of the coherent and the incoherent parts is essential for formation of the spectrum. Just in this situation the effects of multiple scattering of projectile appear. The same is true also for depending on polarization part of the spectral intensity.

In an oriented crystal at motion of an electron near the chain of atoms (the axis) the atom density on the trajectory is much higher than in an amorphous medium. As a result, the parameter characterizing the influence of multiple scattering on the radiation process in a medium in absence of an external field ($\nu_0^2 \sim \varepsilon/\varepsilon_0$) becomes of the order of unity at enough low energy (values of ε_0 for tungsten and germanium are given in Table 1). From the other side, due to high density of atoms at the trajectory near axis, the strong electric field of axis acts on the electron. This action diminishes the radiation formation length and expands the characteristic angles of photon emission and hence weakens the influence of multiple scattering on the radiation process. So, one has to use the general expression for the radiation intensity which takes into account both the crystal effective field (the coherent mechanism) and the multiple scattering (the incoherent mechanism) for study of the characteristics of radiation. Such expression for the unpolarized case $dI_0(\varepsilon, y)$ was obtained in [1] and the polarization term $dI_1(\varepsilon, y)$ derived here (see Eq.(1.3)). The two first terms of decomposition of $dI_\xi(\varepsilon, y)$ over the parameter ν_0^2 define the coherent and incoherent radiation. It should be noted

that in the incoherent contribution the influence of crystalline field is taken into account. Other terms of the decomposition represent influence of the crystalline field on the multiple scattering (on the LPM effect).

Since in an amorphous medium the LPM effect for the whole spectrum can be observed (for heavy elements) only in TeV energy range (see e.g. [7]) the possibility to study the influence of multiple scattering on radiation process in GeV energy range is evidently of great interest.

In the present paper the detailed analysis of the spectral and the polarization properties of radiation is performed. The influence of different mechanisms of photon emission on general picture of event is elucidated. At high energy $\varepsilon \gg \varepsilon_0$ the influence of the multiple scattering on the radiation intensity is suppressed strongly (the coherent contribution dominates) and only in the very end of the spectrum at $u \geq \varepsilon/\varepsilon_0 \gg 1$ ($1 - \omega/\varepsilon \leq \varepsilon_0/\varepsilon \ll 1$) the incoherent radiation becomes essential. In this part of the spectrum the nearly complete (with accuracy $\sim (\varepsilon_0/\varepsilon)^2$) helicity transfer from electron to photon occurs and the scaling defined by Eq.(2.6) takes place. For any energy ε the maximum value of the LPM effect is around 7 % is situated at $u_m \sim 3\varepsilon/\varepsilon_0$ ($\omega_m = \varepsilon u_m/1 + u_m$). For $\omega = \omega_m$ the incoherent contribution dominates, its contribution is one order of magnitude higher than the coherent one. So at $\varepsilon \gg \varepsilon_0$ the maximum of the LPM effect is situated in very end of the spectrum where the mentioned scaling holds. It should be noted the very right end of spectrum is described by the Bethe-Maximon formulae with independent on the electron energy crystal corrections (compare e.g. with Eq.(8) in [1]). For illustration of the discussed effect we considered the low energy $\varepsilon \leq \varepsilon_0$, where both the coherent and incoherent contributions are essential, while the mentioned scaling is only approximate one. This energy region is suitable for experimental study.

The polarization effects in radiation for the intermediate energy is analyzed for the first time. It is shown that the influence of multiple scattering on the polarization part of intensity spectrum $dI_1(\varepsilon, y)$ is very close to the LPM effect in the unpolarized part $dI_0(\varepsilon, y)$.

Acknowledgments

The authors are indebted to the Russian Foundation for Basic Research supported in part this research by Grant 06-02-16226.

Список литературы

- [1] V. N. Baier, and V. M. Katkov, Phys. Lett.,A **353** (2006) 91.
- [2] K. Kirsenom *et al*, Phys. Rev. Lett., **87** (2001) 054801.
- [3] A. Baurichter *et al*, Phys. Rev. Lett., **79** (1997) 3415.
- [4] V. N. Baier, V. M. Katkov, Nucl.Instr.and Meth B, **234** (2005) 106.
- [5] V. N. Baier, V. M. Katkov and V. M. Strakhovenko, *Electromagnetic Processes at High Energies in Oriented Single Crystals*, World Scientific Publishing Co, Singapore, 1998.
- [6] V. N. Baier and V. M. Katkov, Phys.Rev. D **62** (2000) 036008.
- [7] V. N. Baier and V. M. Katkov, Phys.Rep. **409** (2005) 261.

V.N. Baier and V.M. Katkov

**Spectrum and polarization
of coherent and incoherent radiation
and the LPM effect in oriented single crystal**

В.Н. Байер, В.М. Катков

**Спектр и поляризация
когерентного и некогерентного излучения
и ЛПМ эффект в ориентированных монокристаллах**

Budker INP 2007-22

Ответственный за выпуск А.М. Кудрявцев
Работа поступила 4.07.2007 г.

Сдано в набор 12.09.2007 г.

Подписано в печать 12.09.2007 г.

Формат бумаги 60×90 1/16 Объем 1.2 печ.л., 1.0 уч.-изд.л.

Тираж 105 экз. Бесплатно. Заказ № 22

Обработано на IBM PC и отпечатано на
ротапринте ИЯФ им. Г.И. Будкера СО РАН
Новосибирск, 630090, пр. академика Лаврентьева, 11.